Enhancement of the Anti-diabetic Activities of Tea Protein Hydrolysate (TPH) through the Conjugation of TPH with EGCG: Characterization of Conjugate

Sam Al-Dalali[a,b,c,d,*], Xiaozheng Fan[a], Zhigui He[a,b,c], Shamsan A. Almowallad[d]

[a] *School of Food and Health, Guilin Tourism University, Guilin 541006, China*

[b] *Guangxi Engineering Research Center for Large-Scale Preparation & Nutrients and Hygiene of Guangxi Cuisine, Guilin 541006, China*

[c] *Key Laboratory of Industrialized Processing and Safety of Guangxi Cuisine, (Guilin Tourism University), Education Department of Guangxi Zhuang Autonomous Region, China*

[d] *Department of Food Science and Technology, Faculty of Agriculture and Food Science, Ibb University, Ibb 70270, Yemen*

salihsam4@gmail.com

Keywords: *Tea protein hydrolysate (TPH); EGCG-TPH conjugate; EGCG; Antidiabetic activity; FTIR*

This study produced a tea protein hydrolysate (TPH) from Fujian white tea residue at pH 9, with a solid-to-liquid (S/L) ratio of 1:20 *(w/v),* an enzyme-to-substrate (E/S) ratio of 1.188%, a temperature of 60 ℃, and a reaction time of 3 hours. After free-radical grafting, EGCG and TPH formed conjugates. The functional properties of the conjugate and its main components, including solubility, were evaluated. Additionally, UV-visible spectroscopy, Fourier transform infrared spectroscopy (FTIR), and scanning electron microscopy (SEM) were used to confirm the formation of the conjugate. EGCG and TPH formed conjugates, as suggested by FTIR, UV-visible spectroscopy, and SEM analyses, thereby enhancing *in vitro* anti-diabetic enzyme-inhibitory activity. The conjugation of EGCG and TPH increased the inhibition rates of α-amylase and α-glucosidase by 8.1% and 25.4%, respectively, compared to EGCG alone, and by 28.7% and 55.7% compared to TPH alone. Moreover, EGCG-TPH showed improved functional performance over each sample. The synergistic enhancement of the complex's anti-diabetic properties, through free radical scavenging and enzyme inhibition, confirms the structural integrity of the EGCG-TPH conjugate. This mechanism of synergistic activity provides a new approach to developing anti-diabetic compounds from natural sources. It highlights the potential to utilize high-value tea-processing byproducts and support the development of functional dietary strategies for diabetes.

Introduction

Among the leading causes of adult mortality, diabetes mellitus has become a significant global public health issue. It is projected to affect 700 million people by 2045 and is classified as a chronic metabolic disorder [1,2]. Type 2 diabetes mellitus (T2DM) is characterized by the body's inability to produce enough insulin due to impaired beta-cell function and insulin resistance. The disruption of insulin signaling pathways and beta cell function is mainly caused by stress mediated by intracellular reactive oxygen species. Kang et al. note that these pathways are primarily triggered by persistent hyperglycemia and hyperlipidemia [3]. Xia et al. observed that patients with T2DM face additional difficulties due to common side effects linked to various anti-diabetic medications, including gastrointestinal issues, heart failure, and vaginal infections [4]. Therefore, there is a pressing need to develop new antidiabetic functional dietary interventions with fewer adverse effects. Recently, plant proteins have attracted significant attention from researchers because of their safety and effectiveness [5]. Thompson et al. argue that a plant-based diet may lower the risk of T2DM by enhancing liver and kidney function, reducing baseline inflammation, promoting normal blood sugar levels, and decreasing body fat [6].

Enzymatic hydrolysis is commonly used to produce hydrolysates from plant proteins. This process uses enzymes, primarily proteases, to extract a variety of bioactive peptides [7]. Enzymatic hydrolysis is a readily applicable technique for regulating digestive health [8]. By breaking down tea proteins into peptides and free amino acids, proteolytic enzymes enhance their biological activity. In some cases, it also produces relatively consistent hydrolysates. The bioactive qualities, flavor, and uniqueness of different tea products are significantly affected by FAA [9]. Plant protein hydrolysates are an essential source of bioactive compounds and offer an alternative for obtaining proteins and health-promoting ingredients for specialty nutritional products. According to Bajerska et al., various plant proteins and their hydrolyzed peptides show promise in treating diabetes and hypertension, reducing cholesterol, preventing cancer, lowering inflammation, providing antioxidant effects, and reducing the risk of chronic disease [10]. The mechanisms behind the anti-diabetic effects of bioactive peptides include inhibiting α-amylase, α-glucosidase, and DPP-IV, stimulating pancreatic insulin secretion, and improving insulin sensitivity in target tissues [11]. High-protein raw materials are the primary source of natural active peptides. Currently, many peptides with anti-diabetic properties have

been extracted from a range of high-protein food sources. Recent research has highlighted tea protein-derived active peptides, including hypoglycemic [12], antioxidant [13], antihypertensive [14], and lipid-lowering [15] peptides.

China is the leading global producer of tea, producing approximately 200,000 to 300,000 tons of lower-quality crushed tea and tea residue each year. The rise in industrial canned tea beverages has significantly increased the amount of tea residue. Tea residue contains 20%-25% crude protein and may exhibit beneficial biological activity [13]. These proteins can be extracted and converted into valuable products, such as bioactive peptides and protein hydrolysates. Tea protein is a plant-based, cholesterol-free, amino acid-rich protein, making it especially suitable for specific populations [10]. Fujian white tea is a highly valued Chinese tea known for its low level of fermentation. Recent studies have revealed several biological functions of white tea, including its neuroprotective, anti-inflammatory, and anticancer properties [14,16,17].

Epigallocatechin gallate (EGCG) is another crucial active compound found in tea. EGCG has attracted significant attention for its potent bioactivity and potential health benefits. Its diverse properties make interactions with proteins a significant focus of research, especially in other protein-polymer combinations [18]. Although EGCG shows high activity, it is susceptible to oxidation and has low solubility in both aqueous and lipid environments, which limits its use [19]. Conjugating EGCG to other biologically active molecules, such as protein hydrolysates, starches, and oligosaccharides, has provided evidence that it enhances both the stability and the synergistic bioactivity [20]. While there are many documented investigations on protein-polyphenol interactions and also the formation of covalently bonded protein-EGCG conjugates, the specific use of a free radical-initiated grafting reaction to form covalent bonds between EGCG and tea protein hydrolysate (TPH) has not previously been evaluated in detail. The free-radical grafting process enables covalent bonding between EGCG and peptides derived from TPH. It is hypothesized that this will result in altered molecular conformations that expose more hydrophobic regions and hydroxyl groups, and increased functional stability of the formed EGCG-TPH conjugate [18, 21]. Most significantly, past studies primarily examined general protein-polyphenol conjugates and therefore did not investigate how covalent attachment of EGCG to TPH could enhance the synergistic anti-diabetic activity. Therefore, this work bridges an important knowledge gap by

investigating the structural and functional differences of EGCG-TPH conjugates and evaluating their superior anti-diabetic activities compared to unmodified TPH. Characterization of the interaction and structure modifications was evaluated using Fourier Transform Infrared Spectroscopy (FTIR), Scanning Electron Microscopy (SEM), and Ultraviolet-Visible Spectroscopy (UV-vis).

Materials and methods

Experimental materials

The Fujian white tea was sourced from Fuding Huiteng Tea Industry Co., Ltd., in Fujian Province, China. EGCG 98% was obtained from Shanghai Yuanye Biotechnology Co., Ltd. Trypsin (from pig pancreas) (250 U/mg) was purchased from McLean Biochemical Co., Ltd. 2,2-Azidobis (3-ethylbenzothiazoline-6-sulfonic acid) (ABTS) and 1,1-diphenyl-2-picrylhydrazone (DPPH) free radicals were acquired from Sigma Co., Ltd. (Shanghai, China). α-Glucosidase (from yeast) and α-amylase (from pig pancreas) were also sourced from Shanghai Yuanye Biotechnology Co., Ltd. p-Nitrophenyl-α-d-glucopyranoside (PNP Glu) was obtained from Biotoped® Life Sciences.

Experimental methods

Extraction of tea protein

A specific amount of dried white tea leaves was placed in an empty jar and submerged in 1200 mL of boiling water. After 15 minutes of soaking, the water was removed and replaced with fresh boiling water. The soaking process was carried out in three stages. The tea leaves were dried in an electric oven at 100 °C for 4 hours, then ground. The resulting powder was filtered through a 60 μm screen to remove larger particles. The tea powder was extracted using an alkaline solution, a common method for extracting plant proteins. The extraction was performed using a solid-to-liquid ratio of 1:30, with 0.1 mol/L alkali solution, and an extraction duration of 60 minutes at 80 °C. After 60 minutes in the alkaline solution, the tea powder extracts were centrifuged to remove insoluble matter. The protein precipitate was obtained from the tea residue by adjusting the supernatant pH to 3.0–4.0. The protein content of the residue was determined by the Kjeldahl method, and approximately 80% of the tea residue was protein.

Preparation of white tea protein hydrolysate (TPH)

To perform enzymatic hydrolysis, the necessary parameters include: pH 9, substrate concentration (S/L) 1:20 (*w/v*), enzyme-to-substrate ratio (E/S) 1.188, temperature at 60 ℃, and an incubation time of 3 hours. The reaction mixture was thoroughly stirred in an ultrasonic water bath at 40 kHz for the enzymatic hydrolysis of white tea protein samples. Once the

protein sample and sodium phosphate buffer (pH 7.0) reached a specific temperature, the enzyme was added. After the reaction time was complete, the mixture was heated in a water bath at 90–95 °C for 10 minutes to halt enzyme activity. The mixture was then centrifuged at 4400 *g* and 4 ℃ for 20 minutes using an Avanti J-26S XP centrifuge (USA). Post-centrifugation, the supernatant was pre-cooled for 6 hours in an ultra-low-temperature freezer (-80 ℃). Next, it was placed in a vacuum freeze-drying system (FD-2 vacuum freeze dryer: Beijing Boyikang Experimental Instrument Co., Ltd.) and subjected to low-temperature dehydration for 48 hours. The vacuum pressure was maintained at 0.12 mbar, with a condensation temperature of -52 ℃. Before further testing, the freeze-dried powder was carefully sealed in sterile bags and stored at -20 ℃.

Determination of hydrolysis degree

The degree of hydrolysis (DH) of TPH is determined using the pH stabilization method, which measures the amount of sodium hydroxide (NaOH) required to maintain a constant pH during enzymatic hydrolysis. The DH value is calculated using the equation provided by Adler Nissen [22].

$$DH\ (\%) = (BN_b / \alpha h_{tot}\ Mp) \times 100$$

The variables in the equation are defined as follows: h_{tot} represents the total number of peptide bonds per gram of white tea protein (7.13 mM/g protein), B indicates the volume of NaOH used (mL), N_b signifies the NaOH equivalent (0.1N), Mp is the mass of protein in the sample (g), and α reflects the average dissociation level of terminal amino peptides, calculated using the following equation:

$$\alpha = (10^{(pH\text{-}pk)}/1 + 10^{(pH\text{-}pk)})$$

The pH and pK values indicate the conditions for enzymatic protein hydrolysis.

Preparation of TPH-EGCG conjugate

The free-radical grafting procedure described by Chotphruethipong et al. [23] was modified to enhance conjugation between TPH and EGCG. Prepare a TPH solution by dissolving it in distilled water to a concentration of 1% (w/v). Then, add 0.15 g of ascorbic acid and 0.5 mL of 5 M H_2O_2 to promote oxidation, stirring at 25 °C for 2 hours. Add 3% EGCG, based on the weight of TPH, to the oxidation mixture, and stir continuously at 4 °C for 24 hours. Dialyze at 4°C for 24 hours to remove unbound EGCG. The TPH-EGCG conjugate was obtained through freeze-drying. The 3% EGCG concentration was chosen because it optimally provides sufficient EGCG to form covalent bonds with TPH while minimizing oxidative damage and/or excessive aggregation of TPH peptides, which can block active sites. Thus, this concentration should allow for an effective

balance among conjugation yield, structural integrity, and the increased anti-diabetic activity of the conjugated TPH-EGCG.

Antidiabetic activity

Determination of α-amylase inhibition

α-Amylase inhibition was performed using the iodine method (IKl) as described by Bahadori et al. [24]. In standard procedures, 50 µL of *α*-amylase solution (0.8 mg/mL) in phosphate-buffered saline (PBS, pH 7.0, 1 M) is mixed with 25 µL of sample solution in 96-well microplates, then incubated at 37 °C for 10 minutes. After adding 50 µL (0.05%) starch, continue incubation at the same temperature for an additional 10 minutes. Prepare blank samples without alpha-amylase. Terminate the reaction by adding 25 µL of 1 M HCl, followed by the addition of 100 µL of IKI solution. The Infinite M200 PRO (Austria) measures the absorbance of both blank and sample at 630 nm to evaluate the alpha-amylase inhibitory effect, as outlined below.

$$\alpha\text{-amylase inhibition activity (\%)} = \frac{AB-AS}{AS} \text{ x100}$$

Where the *AB* and *AS* represented the absorbance of the blank and the sample, respectively.

Determination of α-glucosidase inhibition

An *α*-glucosidase inhibition assay was performed as described by Megrous et al. [25]. Combine 10 µL of *α*-glucosidase solution (2 U/ml) in PBS (50 mM, pH 7.0) with 20 µL of the sample and incubate at 37 °C for 20 min. 10 µL of 5 mM PNPG dissolved in phosphate buffer solution was added as a substrate to initiate the reaction, followed by incubation for 20 min at 37 ℃. Subsequently, 75 µL of 1.0 M Na_2CO_3 solution was introduced to stop the reaction. Blank samples are produced by combining identical components and substituting the sample with PBS. Measure the absorbance of both the sample and the blank at 405 nm. Determine the *α*-glucosidase inhibition rate by applying the subsequent equation:

$$\alpha\text{-glucosidase inhibitory activity (\%)} = \frac{AB-}{AS} \text{ x100}$$

Verification of Conjugate Degree of Conjugated Compounds

UV absorption rate

The UV absorbance at 280 nm of EGCG, TPH, and the conjugate EGCG-TPH was measured by a UV-compatible microplate spectrophotometer (Infinite M200 PRO, Austria). Samples were dissolved in ultrapure deionized water to a final concentration of 10 mg/mL, vortexed for 30 sec, then centrifuged at 5,000 × g for 10 min at 4 °C. An aliquot of 200 µL was transferred from each sample and the blank deionized water, in triplicate, into a UV-transparent flat-bottom microplate. Absorbance at 280 nm was determined at 25 ± 1 °C, with

baseline zeroing by subtracting the mean absorbance of at least three blank wells from all sample well readings.

Fourier Transform Infrared Spectroscopy (FTIR)

The infrared spectra were obtained with a Thermo Fisher Scientific Nicolet at 25 °C. Evaluations were conducted over the 4000–400 cm^{-1} range. TPH-EGCG conjugates, TPH, and EGCG samples were compacted with potassium bromide. Each spectrum was acquired with 16 scans at a resolution of 4 cm^{-1}. The data were analyzed using OriginPro 2024 (64-bit) SR1, version 10.1.0.178, OriginLab Corporation (USA).

Scanning Electron Microscope (SEM)

Examination of SEM images of freeze-dried TPH-EGCG conjugates, TPH peptides, and EGCG utilizing a Japanese Electron JSM-IT100 scanning electron microscope (JEOL Ltd., Tokyo, Japan). The acceleration beam voltage is 5.00 kV, with a 1000× amplification factor, and the working distances are 8.1 mm and 8.2 mm.

Solubility

To estimate the solubility of the lyophilized EGCG, TPH, and EGCG-TPH, the procedure described by Wang et al. [26] was used with some modifications. In short, 25 mL of deionized water (DW) was used to solubilize 100 mg of each sample, and the pH levels were adjusted to 2, 4, 6, 8, and 10 using 0.1 N NaOH or HCl solutions. After 4 min of high-speed mixing, the mixture was centrifuged at 2800 *g* for 10 minutes. Subsequently, the supernatants were dried in weighted dishes for 4 h at 105 °C. Finally, the following formula was applied to determine the solubility:

$$\text{Solubility (\%)} = \frac{W2}{w1} \text{ x } 100$$

W1 and W2 are the weight (mg) of the dissolved sample and the dried supernatant, respectively.

Data analysis

Three independent repeated measurements collected the experimental indicators, and the findings are reported as mean ± SD. For statistical inference, this study employed one-way analysis of variance (ANOVA) paired with Duncan's multiple-comparison test, with *p*-values < 0.05 considered statistically significant. The complete data processing was performed using SPSS 22.0 (SPSS Inc., Chicago, IL, USA).

Results and discussion

Hydrolysis degree (DH)

The Fujian white tea protein hydrolysates were produced by enzymatic hydrolysis, and their degree of hydrolysis (DH) was measured at 30.79±1.08, indicating the extent of structural alteration of tea proteins by proteolytic enzymes. A high DH indicates that trypsin efficiently cleaves peptide bonds in tea proteins, thereby

fragmenting macromolecular proteins into smaller peptides and amino acids. The measured DH demonstrates that this approach effectively degrades tea proteins into smaller peptides, thereby releasing a larger quantity of bioactive peptides.

Anti-diabetes ability of the conjugate and its components

The significance of *α*-amylase in digesting dietary starch is considerable, as it breaks it down into oligosaccharides. α-Glucosidase is an enzyme that catalyzes the hydrolysis of oligosaccharides and disaccharides into glucose; it is found in the small intestinal epithelium [18]. As a result, diabetes and related conditions, including obesity and hypertension, can be effectively managed by inhibiting these enzymes [27]. To boost TPH's anti-diabetic activity, it was conjugated with EGCG. Acarbose was used as a positive control for *α*-glucosidase and *α*-amylase inhibition, yielding an IC_{50} of 0.37 and 4.21 mg/mL, respectively. **Table 1** shows that EGCG-TPH (IC_{50} 0.47) exhibits the most effective inhibition of *α*-glucosidase ($p<0.05$), outperforming EGCG (IC_{50} 0.63) and TPH (IC_{50} 1.06). The inhibition of *α*-glucosidase by TPH-EGCG conjugate exhibited an IC_{50} slightly lower than that of acarbose. Similarly, for *α*-amylase inhibition, EGCG-TPH demonstrates superior efficacy (IC_{50} 5.35; $p<0.05$) compared to EGCG (IC_{50} 5.82) and TPH (IC_{50} 7.5). The inhibition of *α*-amylase by TPH-EGCG conjugate exhibited an IC_{50} slightly lower than that of acarbose. As a catechin flavonoid, EGCG exhibits greater enzyme inhibition than TPH, indicating a higher potential for anti- diabetic effects. Conversely, TPH's inhibitory activity appears to be limited, suggesting that higher concentrations or additional components may be needed to enhance its effectiveness. The EGCG-TPH complex showed the lowest IC_{50} in both assays, with its inhibitory effect significantly surpassing that of the individual components. This indicates that EGCG and TPH may enhance inhibition through a synergistic mechanism. The α-glucosidase inhibition activity of the complex increased by approximately 25.4% relative to EGCG and about 55.7% compared to TPH. The α-amylase inhibition assay revealed that the complex's activity increased by approximately 8.1% relative to EGCG and by approximately 28.7% relative to TPH. Gautam et al. [18] reported that the highest inhibition against α-glucosidase, α-amylase, and pancreatic lipase occurred in conjugation with 6% polyphenols. Interactions between bioactive peptides and digestive enzymes can enhance their efficacy across various medical applications, including blood sugar management and protection of cells from oxidative stress [28]. The potent enzyme

inhibition by the conjugate suggests that it forms stable interactions with the enzyme's active sites, disrupting catalytic activity and reducing carbohydrate and lipid breakdown [18]. In diabetes management, the ability of conjugates to inhibit α-glucosidase and α-amylase is crucial, as these enzymes directly hydrolyze starches and disaccharides into glucose.

Because structural changes disrupt the enzyme's normal function, inhibitory activity increases due to stronger binding interactions. The strongest inhibition was observed with conjugates, likely because of their high binding affinity for the enzyme's active site [18]. These results align with those of Rasouli et al. [29], who screened polyphenols for inhibition of α-amylase and α-glucosidase and found that catechin may inhibit α-amylase. Similarly, Uraipong et al. [30] observed that rice bran protein hydrolysates showed α-amylase inhibitory activity. This suggests that polyphenols, particularly hydrolyzed peptides and EGCG, could serve as natural inhibitors of α-amylase and α-glucosidase.

Gautam et al. [18] studied the conjugation of Pacific white shrimp shell protein hydrolysates with polyphenolic compounds. They found that among all the polyphenols tested, gallic acid conjugates had the highest conjugation efficiency. This is likely due to the lower molecular weight of gallic acid compared to catechin and EGCG, which reduces its tendency to hinder covalent bonding with the large radical sites of the hydrolysates. Differences in conjugation efficiency are often related to variations in phenolic content, the number of free radical-binding sites, and molecular weight.

Table 1. IC50 (mg/mL) of anti-diabetes activities of EGCG-TPH conjugate and its main components

Enzymes	EGCG	TPH	EGCG-TPH
α-Glucosidase Inhibition	0.63^{b}±0.02	1.06^{a}±0.08	0.47^{c} ±0.01
α-Amylase Inhibition	5.82^{b}±0.15	7.5^{a}±0.11	5.35^{c}±0.16

Values are mean ± SD (n=3). EGCG: Epigallocatechin gallate; TPH: Tea protein hydrolysate; EGCG-TPH: conjugate. The different letters indicate statistically significant differences among groups (p<0.05) in each row.

UV-visible spectroscopy

UV absorption can indicate the exposure of tyrosine, tryptophan, and phenylalanine residues [31]. The UV absorbance spectra of EGCG, TPH, and the conjugated compound of EGCG-TPH, shown at 280 nm, are illustrated in **Figure 1**. In terms of the absorbance of free EGCG, there was clearly an extremely high value (~1.52), in line with the established high UV absorbance that occurs due to the large number of aromatic rings,

including the galloyl groups on the catechin backbone [32]. The absorbance of TPH (~0.95) when used separately was considerably lower than that of free EGCG and can be attributed to the UV-absorbing properties of the aromatic amino acids in the TPH chain, specifically tryptophan (~280 nm) and tyrosine (~274 nm) [33]. Of most importance, however, the absorbance for the EGCG-TPH conjugate was found to be higher than that of either of the separate compounds ($p < 0.05$), which is what one would expect given the addition of EGCG's polyphenolic chromophores and TPH's aromatic amino acids in one covalently linked compound together with any new chromophores created by the free radical-initiated grafting reaction [34]. Furthermore, the increasing absorbance values from TPH < EGCG < EGCG-TPH demonstrated the incorporation of EGCG into the backbone of TPH through a covalent linkage, as the absorbance of the conjugate was greater than that expected if they had been mixed as non-covalent entities, indicating a modification of the structure of the compounds and/or redistribution of chromophores brought about by the conjugation process [35].

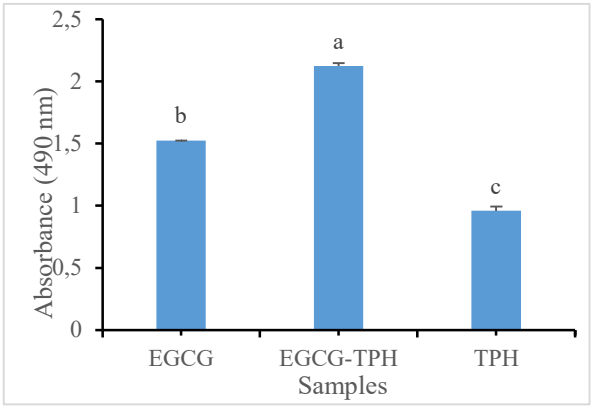

Figure 1. UV absorption of EGCG-TPH conjugate, EGCG, and TPH samples. Values are mean ± SD (n=3). EGCG: Epigallocatechin gallate; TPH: Tea protein hydrolysate; EGCG-TPH: conjugate. The different letters indicate statistically significant differences among groups ($p<0.05$).

Fourier Transform Infrared Spectroscopy (FTIR)

The chemical interactions and structural changes of TPH during conjugation with EGCG were studied by FTIR spectroscopy. This method helps to identify which functional groups are involved and details the nature of the interactions that stabilize the conjugate [36]. FTIR spectra of free EGCG, TPH, and EGCG-TPH conjugate are shown in **Figure 2**. The FTIR spectral comparison provides sufficient evidence of successful covalent attachment between EGCG and TPH. In the high wavenumber region (3500–3200 cm^{-1}), free EGCG exhibited a strong broad absorption band due to O-H stretching of its eight phenolic hydroxyl groups participating in extensive intermolecular hydrogen bonding. In contrast, TPH showed a narrower N-H stretching

band at ~3300 cm^{-1} corresponding to amide A vibrations of the peptide backbone. This region exhibited an enhanced H-bonding between hydroxyl groups of EGCG and protein matrix after the formation of covalent attachment, which correlated with enhanced composite O-H/N-H contributions in EGCG-TPH conjugate. Diagnostic changes were observed in amide I (1700-1600 cm−1) and amide II (1600-1500 cm−1) regions. Specifically, both bands showed measurable shifts in peak position and broader band shape. Specifically, the amide I band shifting to lower wavenumber and the amide II band broadening considerably are directly related to the covalent engagement of free amino groups ($-NH_2$) of lysine residues and *N*-terminal amines through radical-mediated C-N bond formation with EGCG-derived intermediates, which alter the electron density distribution around adjacent peptide units C-O and N-H bonds, leading to modified vibrational frequencies.

In addition, **Figure 2** shows a decrease in EGCG-TPH transmittance relative to TPH in the 3700-3200 cm^{-1} wavenumber range, accompanied by a noticeable increase in spectral intensity. This means the EGCG molecules were covalently bonded with TPH. The EGCG-TPH spectrum in the range of 1000-1500 cm^{-1} shows prominent vibrations mainly attributed to C=O stretching. Moreover, the complex exhibits distinct vibrational modes that indicate the fingerprints of conjugate formation. The shift in characteristic absorption peaks indicates interaction between EGCG and TPH, suggesting that the free-radical grafting method used in the conjugate synthesis has altered the conjugate's secondary structure, resulting in the formation of new peaks. The FTIR spectra (4000-400 cm^{-1}) analysis of the EGCG-TPH conjugate showed the probable covalent interaction where the ester groups of EGCG covalently reacted with the amino groups of TPH via amide bonds (1650/1550 cm^{-1}) after hydrolysis. The shift of the C-O bond in the fingerprint region (e.g., 1250-1265 cm^{-1}) and the change in the characteristic peak of TPH further confirm the formation of a conjugate and an increase in intermolecular interactions. This analysis reveals the possibility of structural interactions between EGCG and TPH that could help elucidate the structure-function relationship of these conjugates. The amide I and II peaks showed differences between the systems, consistent with the literature on polyphenol-protein binding [39]. The peaks of aromatic C=C stretching at ~ 1600 cm^{-1} and phenolic C-O stretching at ~ 1450-1200 cm^{-1} confirmed the conjugated structure of EGCG [32]. In addition to these bands above 1500 cm^{-1}, the fingerprint region below 1000 cm^{-1} was attributed to aromatic C-H bending bands

from gallate and catechin ring substitution patterns in free EGCG. In FTIR spectra, the amide bands (1500-1700 cm^{-1}) mainly indicate C=O stretching, C-N stretching, and N-H bending. Similarly, the peak in the 2800-3000 cm^{-1} range corresponds to C-H stretching vibrations, commonly seen in aliphatic compounds [36]. The peak around 1600 cm^{-1} is typical of N-H bending vibrations in primary amines and suggests the presence of protein-derived functional groups, such as amines and amides [37]. The absorption peak at 3200-3400 cm^{-1} primarily represents the stretching vibrations of O-H and N-H groups [36].

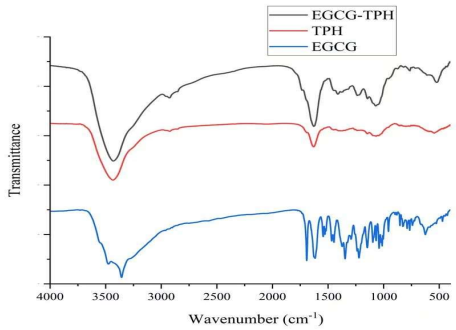

Figure 2. Fourier transform infrared spectra (FTIR) of EGCG-TPH conjugate, EGCG, and TPH samples. EGCG: Epigallocatechin gallate; TPH: Tea protein hydrolysate; EGCG-TPH: conjugate.

Scanning electron microscope

SEM was used to examine and assess the microstructure of the EGCG, TPH, and EGCG-TPH conjugate. EGCG showed a characteristic sheet-like or fibrous structure at 10,000× magnification (**Figure 3b**), with a smooth surface and well-defined edges. The high-resolution image at 1 μm scale revealed uniformly spread nanoscale pores (**Figure 3a**). In contrast, the SEM images of TPH (**Figures 3c and 3d**) depicted a spherical or quasi-spherical particle shape, with a narrow particle size range and increased surface roughness, likely related to the intermolecular forces and crystallization properties of TPH. The SEM images (**Figures 3e and 3f**) of the TPH-EGCG conjugate show significant differences compared to those of the individual components, indicating successful bonding between TPH and EGCG. At 10,000× magnification (**Figure 3e**), the conjugate displays a porous network, with TPH particles embedded within the layered EGCG structure. The low-magnification image (**Figure 3f**) at x1000 demonstrates the overall morphological consistency of the conjugate, suggesting that the composite process did not cause significant phase separation. The structure likely results from interactions between the phenolic hydroxyl groups of EGCG and the active groups of TPH. These interactions enhance mechanical stability and increase the material's specific surface area [18]. The surface roughness of the conjugate in the high-magnification image (x10000) is significantly higher than that of the individual components, possibly linked to its improved adsorption or reaction activity. The features show

similarities and a higher density than TPH. This process decreases surface hydrophobicity and aligns hydrophilic groups with hydrophobic protein components, leading to multiple binding and aggregation phenomena. The morphological features suggest that the TPH-EGCG conjugate combines the structural advantages of both components. The SEM microstructure clearly shows the structural complementarity and morphological traits of the conjugate. Peptides are increasingly advantageous due to their small size, allowing each nanoparticle to bind more peptide molecules [38]. It also suggests that other active compounds, such as EGCG, quercetin, and resveratrol, might boost their effectiveness by binding to TPH.

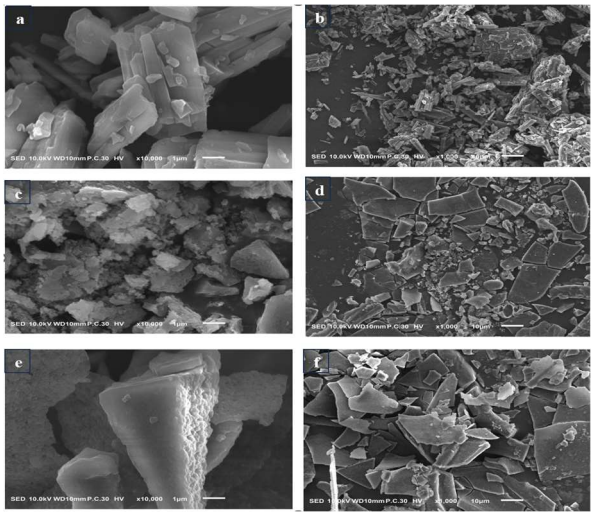

Figure 3. SEM of EGCG (a and b), TPH (c and d), and TPH-EGCG conjugate (e and f) at different magnifications: X10,000 and X1000, respectively. EGCG: Epigallocatechin gallate; TPH: Tea protein hydrolysate; EGCG-TPH: conjugate.

Solubility

Solubility is a key property that affects various protein functions across different food-system applications. The binding of polyphenols to proteins can impact protein solubility, depending on the system's characteristics [39]. The pH-dependent solubility behaviors of EGCG, TPH and the EGCG-TPH conjugate are shown in **Figure 4** and indicated that free EGCG had relatively stable and high solubility (94.8±3.6% to 99.7±3.5%) from pH 2 to 10 with no statistical difference (p>0.05), which was attributed to its eight hydroxyl group containing galloyl and catechol ring structures capable of forming large amounts of hydrogen-bonded networks with H_2O molecules under all pH values, thus, resulting in the strong pH-independency of its hydrophilicity independent of the protonation state of nearby residues [32]. In contrast, TPH demonstrated the greatest pH-dependent behavior among the three samples examined here, with the lowest measured solubility of 65.2±0.85% occurring at pH 2 (p<0.05 when compared to each other's pH values), a second low solubility of 76.3±2.6% at pH 8, and the highest solubility of 99.8±2.8% at pH 6. Similar trends have been reported previously in the literature regarding protein hydrolysate solubility, where the minimum solubility generally occurs around the protein isoelectric point due to diminished electrostatic

repulsive forces between peptide chains and increased hydrophobic aggregation/association through exposed nonpolar residues; however, increasing levels of electrostatic repulsion via net charges on peptides at either acidic or basic pH will increase solubility [39]. The solubility values obtained for the EGCG-TPH conjugate ranged from 82.1±2.4% at pH 2, 89.3±3.4% at pH 4, 99.1±1.9% at pH 6, 89.2±2.2% at pH 8, and 94.4±2.5% at pH 10. The solubilities of these compounds are statistically higher than those of unconjugated TPH at pH 2, 4, 8, and 10 ($p < 0.05$), but lower than those of unconjugated EGCG at the same pH levels. This indicates that the shape of the conjugate has been affected in two different ways: (1) the grafting of EGCG onto TPH peptide chains adds hydrophilic hydroxyl groups to the TPH surface, disrupts ordered hydrophobic regions, and increases steric repulsion between peptide chains, thereby improving the solubility of the conjugate relative to unconjugated TPH; (2) however, this grafting reaction consumes some of the available positively charged amino groups (-NH2) on the surface of TPH, reducing electrostatic repulsion that contributes to maintaining soluble states at extreme pH values; furthermore, new C-N and C-C covalent linkages formed between the phenolic EGCG and TPH introduce rigidity to local peptide fragments of the protein, which can lead to organized hydrophobic packing and reduced solubility of the conjugate relative to unconjugated EGCG; especially since many, if not all, of the free amino groups lost upon reaction are involved in maintaining soluble states within their native environments [41; 34; 35). This increased solubility indicates that conjugation enhances the peptide's functional and biological properties related to solubility. These findings agree with those reported by Benjakul et al. [40], who observed that the functional characteristics of proteins decline due to precipitation and aggregation at higher concentrations. The solubility of conjugates is significantly influenced by the pH at which their interactions occur, as well as the types of polyphenols and proteins involved [39]. Covalent grafting of EGCG seems to be an interesting approach to improve the pH stability of tea protein hydrolysate, especially in acidic food systems (pH 2–4) such as beverages, dressings, and fermented products, where protein solubility is often difficult to maintain. The overall solubility of EGCG-TPH was significantly higher than that of free TPH at both acidic and alkaline pH ($p < 0.05$).

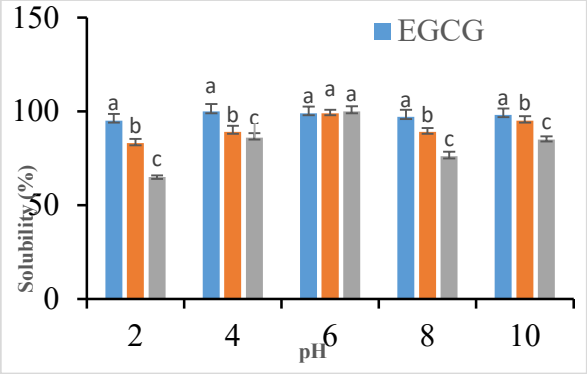

Figure 4. Solubility of EGCG-TPH conjugate, EGCG, and TPH at different pH levels. Values are mean ± SD (n=3). EGCG: Epigallocatechin gallate; TPH: Tea protein hydrolysate; EGCG-TPH: conjugate. The different letters indicate statistically significant differences among groups ($p < 0.05$) at each pH.

Conclusion

The optimal conditions for producing TPH from Fujian white tea protein were S/L: 20, E/S: 1.188, and pH 9. The combination of EGCG and TPH significantly enhanced the compound's inhibitory activity against α-amylase and α-glucosidase, thereby increasing its potential for development as a functional food ingredient targeting glucose metabolism. Activity assessment showed that the inhibitory effectiveness of the EGCG-TPH complex on α-amylase and α-glucosidase increased by 8.1% and 25.4%, respectively, compared with EGCG alone. Compared to TPH alone, the increases were approximately 28.7% and 55.7%, respectively. This study used FTIR, UV-visible spectroscopy, and SEM to reveal the conjugation reaction between EGCG and TPH, providing strong evidence of successful product coupling. Incorporating TPH with EGCG shifted the inhibitory effect from a single component to a multi-component synergy, offering a new strategy for developing functional food ingredients with *in vitro* anti-diabetic potential. The findings demonstrate that combining these two substances is entirely feasible and that the conjugate exhibits improved functional characteristics under the conditions studied.

Acknowledgments

This study was supported by the High-level Talent Research Funds of Guilin Tourism University (C00424002) and the Innovation and Entrepreneurship Training Program for College Students at Guilin Tourism University (S202411837033).

References

[1] Li P, Cao T, Li Z, Li W. Identification and antidiabetic activity of peptides in protein Morus alba leaf proteolytic hydrolysates: A novel functional food ingredient for ameliorating type 2 diabetes mellitus. Food Bioscience 2025;66:106139.

[2] Peng D, Tian W, An M, Chen Y, Zeng W, Zhu S, Li P, Du B. Characterization of antidiabetic effects of Dendrobium officinale derivatives in a mouse model of type 2 diabetes mellitus. Food Chemistry 2023;399:133974.

[3] Kang G, Francis N, Hill R, Waters D, Blanchard C, Santhakumar A. Dietary Polyphenols and Gene Expression in Molecular Pathways Associated with Type 2 Diabetes Mellitus: A Review. International Journal of Molecular Sciences 2019;21(1):140.

[4] Xia T, Liu C, Hu Y, Luo Z, Chen F, Yuan L, Tan X. Coix seed polysaccharides alleviate type 2 diabetes mellitus via gut microbiota-derived short-chain fatty acids

activation of IGF1/PI3K/AKT signaling. Food Research International 2021;150:110717.

[5] Yang X, Wang Y, Tang X, Wei J, Yu X, Kang J, Xi Y, Xue X. Corni Fructus extracts ameliorate Streptozotocin-Induced diabetes in mice via regulating AMPK/ACC/CPT-1 signaling pathway. Journal of Functional Foods 2023;107:105661.

[6] Thompson A, Candussi C, Tresserra-Rimbau A, Jennings A, Bondonno N, Hill C, Sowah S, Cassidy A, Kühn T. A healthful plant-based diet is associated with lower type 2 diabetes risk via improved metabolic state and organ function: A prospective cohort study. Diabetes & Metabolism 2024;50(1):101499.

[7] Kumar M, Selvasekaran P, Chidambaram R, Zhang B, Hasan M, Prakash Gupta O, Rais N, Sharma K, Sharma A, Lorenzo J, Parameswari E, Deshmukh V, Elkelish A, Abdel-Wahab B, Chandran D, Dey A, Senapathy M, Singh S, Pandiselvam R, Sampathrajan V, Dhumal S, Amarowicz R. Tea (Camellia sinensis (L.) Kuntze) as an emerging source of protein and bioactive peptides: A narrative review. Food Chemistry 2023;428:136783.

[8] Yao G, He W, Wu Y, Chen J, Hu X, Yu J. Purification of Angiotensin-I-Converting Enzyme Inhibitory Peptides Derived from Camellia oleifera Abel Seed Meal Hydrolysate. Journal of Food Quality 2019;2019:1-9.

[9] Shi Y, Zhu Y, Ma W, Shi J, Peng Q, Lin Z, Lv H. Comprehensive investigation on non-volatile and volatile metabolites in four types of green teas obtained from the same tea cultivar of Longjing 43 (Camellia sinensis var. sinensis) using the widely targeted metabolomics. Food Chemistry 2022;394:133501.

[10] Bajerska J, Wozniewicz M, Jeszka J, Drzymala-Czyz S, Walkowiak J. Green tea aqueous extract reduces visceral fat and decreases protein availability in rats fed with a high-fat diet. Nutrition Research 2011;31(2):157-164.

[11] Antony P, Vijayan R. Bioactive Peptides as Potential Nutraceuticals for Diabetes Therapy: A Comprehensive Review. International Journal of Molecular Sciences 2021;22(16):9059.

[12] Zhao B, Su K, Mao X, Zhang X. Separation and identification of enzyme inhibition peptides from dark tea protein. Bioorganic Chemistry 2020;99:103772.

[13] Zhao L, Wang S, Huang Y. Antioxidant function of tea dregs protein hydrolysates in liposome–meat system and its possible action mechanism. International Journal of Food Science & Technology 2014;49(10):2299-2306.

[14] Zhou S, Zhang J, Ma S, Ou C, Feng X, Pan Y, Gong S, Fan F, Chen P, Chu Q. Recent advances on white tea: Manufacturing, compositions, aging characteristics and bioactivities. Trends in Food Science & Technology 2023;134:41-55.

[15] Ye H, Xu Y, Sun Y, Liu B, Chen B, Liu G, Cao Y, Miao J. Purification, identification and hypolipidemic activities of three novel hypolipidemic peptides from tea protein. Food Research International 2023;165:112450.

[16] Zhang J, Xin W, Zou Y, Yan J, Tang W, Ji Y, Li W. Dynamic changes and correlation analysis of microorganisms and flavonoids/ amino acids during white tea storage. Food Chemistry 2024;455:139932.

[17] Zhang Z, Sun L, Chen R, Li Q, Lai X, Wen S, Cao J, Lai Z, Li Z, Sun S. Recent insights into the physicochemical properties, bioactivities and their relationship of tea polysaccharides. Food Chemistry 2024;432:137223.

[18] Gautam A, Benjakul S, Kadam D, Tiwari B, Singh A. Enhanced Antioxidant and Digestive Enzyme Inhibitory Activities of Pacific White Shrimp Shell Protein Hydrolysates via Conjugation with Polyphenol: Characterization and Application in Surimi Gel. Foods 2024;13(24):4022.

[19] Liu X, Song Q, Li X, Chen Y, Liu C, Zhu X, Liu J, Granato D, Wang Y, Huang J. Effects of different dietary polyphenols on conformational changes and functional properties of protein–polyphenol covalent complexes. Food Chemistry 2021;361:130071.

[20] Huang R, Mendis E, Kim S. Improvement of ACE inhibitory activity of chitooligosaccharides (COS) by carboxyl modification. Bioorganic & Medicinal Chemistry 2005;13(11):3649-3655.

[21] Feng Y, Jin C, Lv S, Zhang H, Ren F, Wang J. Molecular Mechanisms and Applications of Polyphenol-Protein Complexes with Antioxidant Properties: A Review. Antioxidants 2023;12(8):1577.

[22] Adler-Nissen J. Enzymic hydrolysis of proteins for increased solubility. Journal of Agricultural and Food Chemistry 1976;24(6):1090-1093.

[23] Chotphruethipong L, Hutamekalin P, Sukketsiri W, Benjakul S. Effects of sonication and ultrasound on properties and bioactivities of liposomes loaded with hydrolyzed collagen from defatted sea bass skin conjugated with epigallocatechin gallate. Journal of Food Biochemistry 2021;45(8):e13809.

[24] Bahadori M, Dinparast L, Zengin G, Sarikurkcu C, Bahadori S, Asghari B, Movahhedin N. Functional components, antidiabetic, anti-Alzheimer's disease, and antioxidant activities of Salvia syriaca L. International Journal of Food Properties 2016;20(8):1761-1772.

[25] Megrous S, Al-Dalali S, Zhao X, Chen C, Cao Y, Bourouis I, Mekkaoui A, Yang Z, Yang Z. Evaluation of Antidiabetic Activities of Casein Hydrolysates by a Bacillus Metalloendopeptidase. International Journal of Peptide Research and Therapeutics 2020;26(4):2519-2527.

[26] Wang Y, Noman A, Zhang C, Al-Dalali S, Abed S. Effects of ultrasound pretreatment on the enzymolysis of hybrid sturgeon (Huso dauricus × Acipenser schrenckii) protein and the structural, functional, and antioxidant properties of hydrolysates. Lwt 2023;188:115421.

[27] Awosika T, Aluko R. Inhibition of the in vitro activities of α-amylase, α-glucosidase and pancreatic lipase by yellow field pea (Pisum sativum L.) protein hydrolysates. International Journal of Food Science & Technology 2019;54(6):2021-2034.

[28] Daliri E, Oh D, Lee B. Bioactive Peptides. Foods 2017;6(5):32.

[29] Rasouli H, Hosseini-Ghazvini S, Adibi H, Khodarahmi R. Differential α-amylase/α-glucosidase inhibitory activities of plant-derived phenolic compounds: a virtual screening perspective for the treatment of obesity and diabetes. Food & Function 2017;8(5):1942-1954.

[30] Uraipong C, Zhao J. Rice bran protein hydrolysates exhibit strong in vitro α-amylase, β-glucosidase and ACE-inhibition activities. Journal of the Science of Food and Agriculture 2015;96(4):1101-1110.

[31] Du P, Tu Z, Wang H, Hu Y. Mechanism of Selenium Nanoparticles Inhibiting Advanced Glycation End Products. Journal of Agricultural and Food Chemistry 2020;68(39):10586-10595.

[32] Liu J, Yong H, Yao X, Hu H, Yun D, Xiao L. Recent advances in phenolic–protein conjugates: synthesis, characterization, biological activities and potential applications. RSC Advances 2019;9(61):35825-35840.

[33] Simonian M. Spectrophotometric Determination of Protein Concentration. Current Protocols in Cell Biology 2002;15(1).

[34] Zhang K, Huang J, Wang D, Wan X, Wang Y. Covalent polyphenols-proteins interactions in food processing: formation mechanisms, quantification methods, bioactive effects, and applications. Frontiers in Nutrition 2024;11:1371401.

[35] Li X, Li M, Zhang T, McClements D, Liu X, Wu X, Liu F. Enzymatic and Nonenzymatic Conjugates of Lactoferrin and (−)-Epigallocatechin Gallate: Formation, Structure, Functionality, and Allergenicity. Journal of Agricultural and Food Chemistry 2021;69(22):6291-6302.

[36] Bourouis I, McClements D, Li H, Pang Z, Liu X. Interaction mechanism between soy protein microgels and chitosan and the resulting physical properties: effect of biopolymer ratio, pH and ionic strength. Food Hydrocolloids 2025;168:111557.

[37] Kong J, Yu S. Fourier Transform Infrared Spectroscopic Analysis of Protein Secondary Structures. Acta Biochimica et Biophysica Sinica 2007;39(8):549-559.

[38] Sankar V, Devi Penmetsa S, Sabarinath C. Folate Conjugated Solid Lipid Nanoparticles of Carboplatin for Targeting Cancer Cells. Drug Delivery Letterse 2012;2(3):162-170.

[39] Quan T, Benjakul S, Sae-leaw T, Balange A, Maqsood S. Protein–polyphenol conjugates: Antioxidant property, functionalities and their applications. Trends in Food Science & Technology 2019;91:507-517.

[40] Benjakul S, Singh A, Chotphruethipong L, Mittal A. Protein-polyphenol conjugates: Preparation, functional properties, bioactivities and applications in foods and nutraceuticals. Advances in Food and Nutrition Research 2021;98:281-320.

[41] Yan S, Wang Q, Yu J, Li Y, Qi B. Ultrasound-assisted preparation of protein–polyphenol conjugates and their

structural and functional characteristics. Ultrasonics Sonochemistry 2023;100:106645.